Figures and figure supplements

Quantitative uniqueness of human brain evolution revealed through phylogenetic comparative analysis

Ian F Miller *et al*
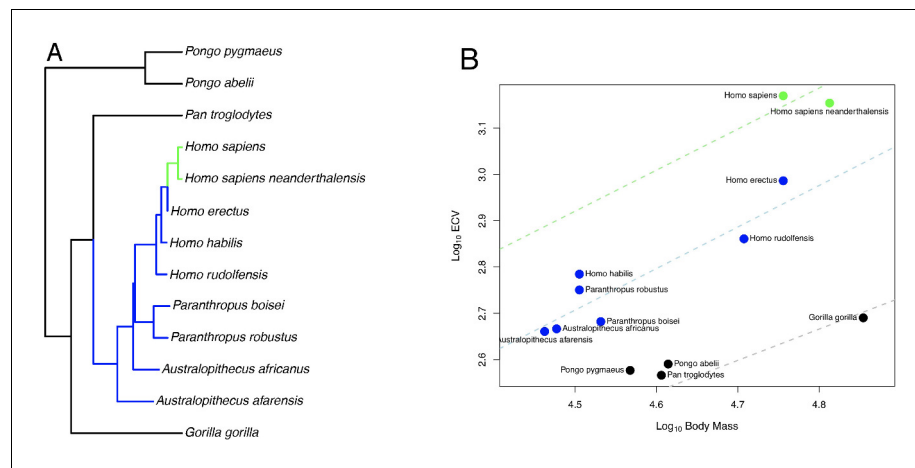
Figure 1. OU Model of ECV Evolution in Primates Panel. A shows the location of the selection regimes identified in an OU model of ECV predicted by body mass. Panel B shows the corresponding optimum regression lines representing the various selection regimes, along with body mass and ECV data. Data are colored by their corresponding selection regimes. All results are from the un-weighted predictor OU model in the bayou analysis using the alternate hominin phylogeny. Only the great ape clade is shown; selection regimes across the entire primate phylogeny are show in *Figure 1—figure supplement 1*.

DOI: https://doi.org/10.7554/eLife.41250.006
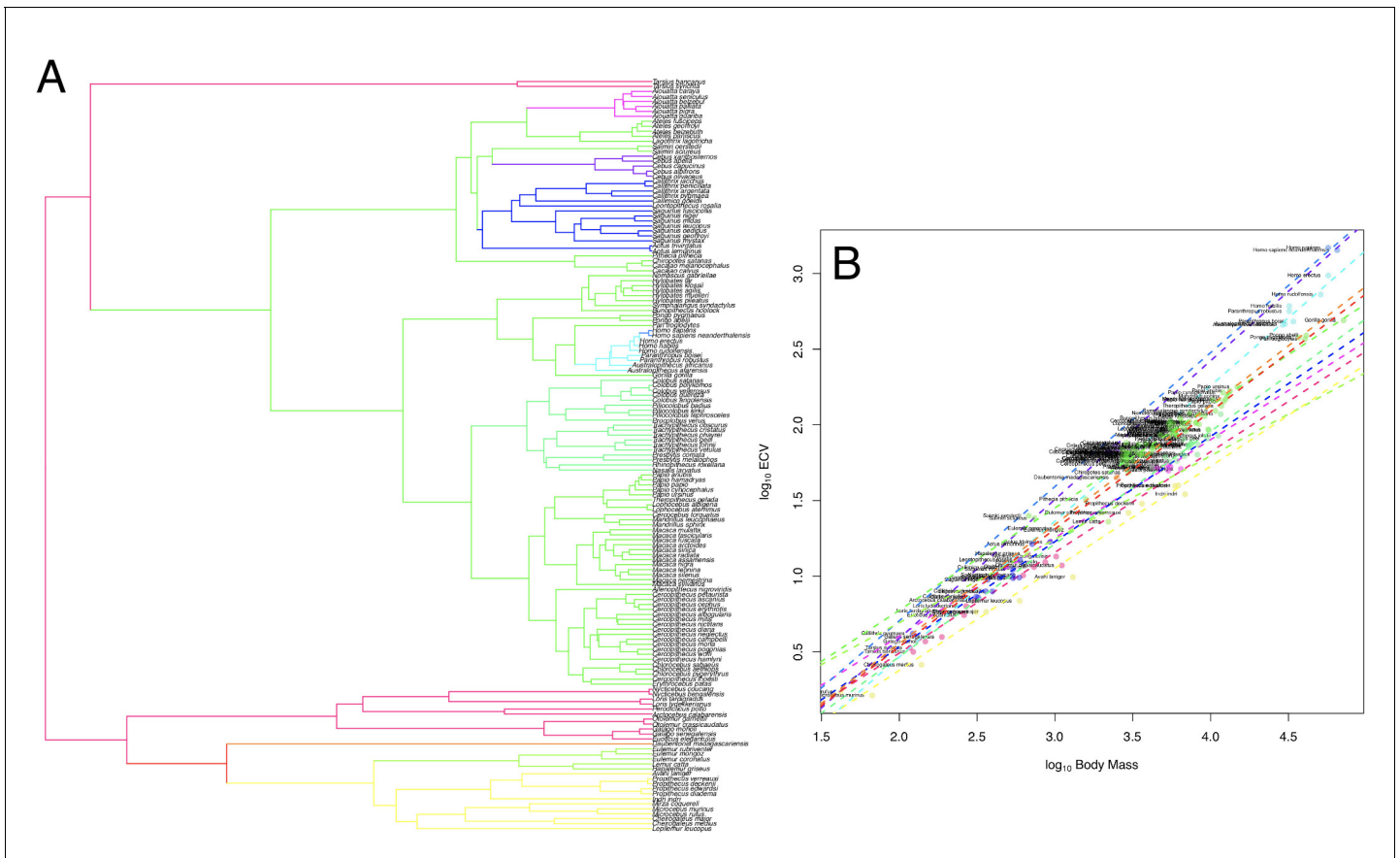
Figure 1—figure supplement 1. OU Model of ECV Evolution in Primates Results are shown for the un-weighted predictor OU model of ECV predicted by body mass. *Figure 1* displays the same results, but only for great apes. Panel A shows the location of the selection regimes. Panel B shows the optimum regression lines representing the various selection regimes, along with body mass and ECV data. Data in panel B are colored according to the corresponding regimes shown in panel A.

DOI: https://doi.org/10.7554/eLife.41250.007
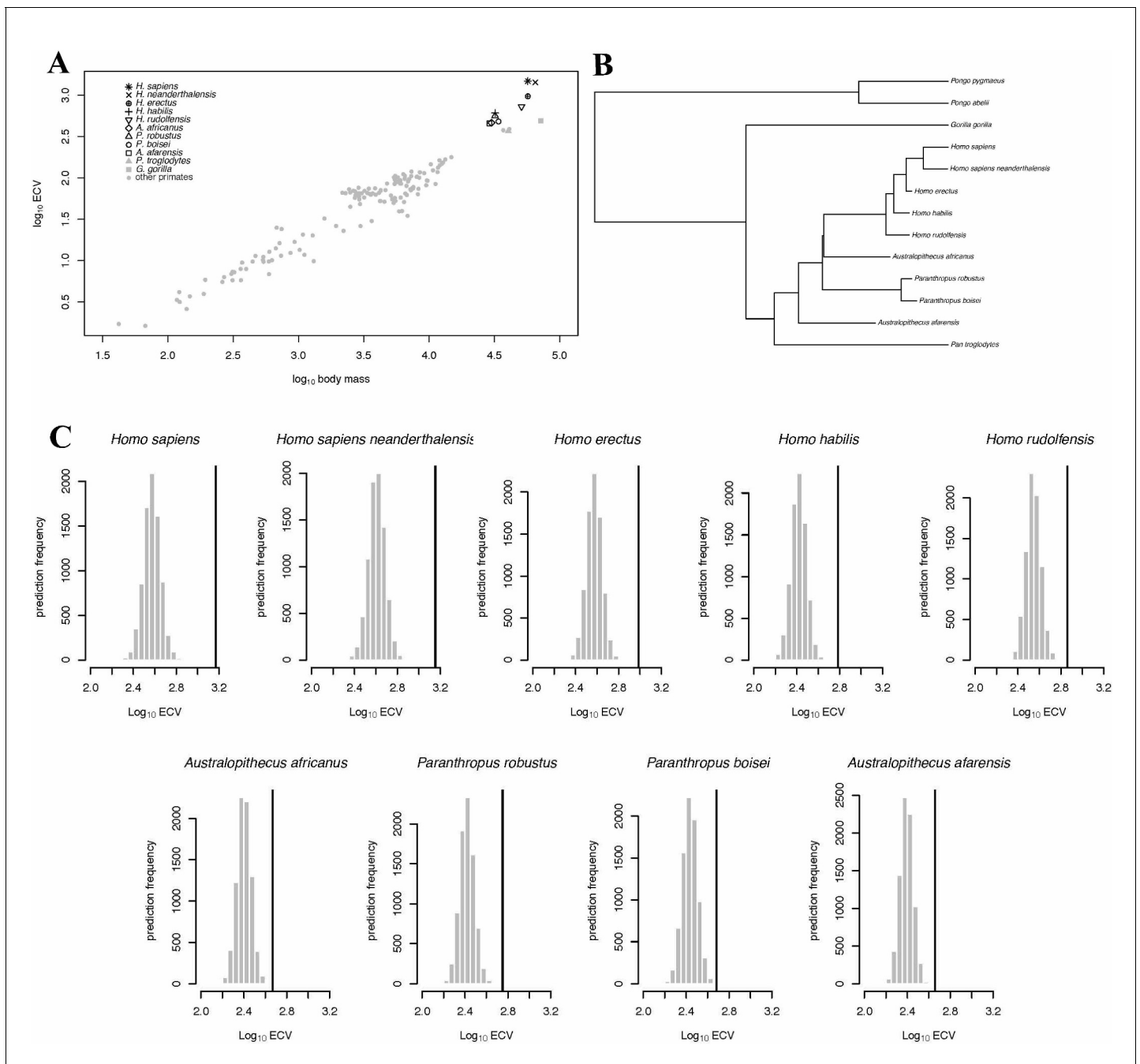
Figure 2. BayesModelS predictions of ECV in hominins. Panel (A) shows a scatter plot of primate ECV and body mass data. Panel (B) shows the topology of the great ape portion of the hominin phylogeny used in the BayesModelS analyses of hominin ECV. Panel (C) shows the posterior distributions of predicted ECV values generated by BayesModelS for hominin species with body mass used as the predictor variable. Vertical lines indicated observed values.

DOI: https://doi.org/10.7554/eLife.41250.008
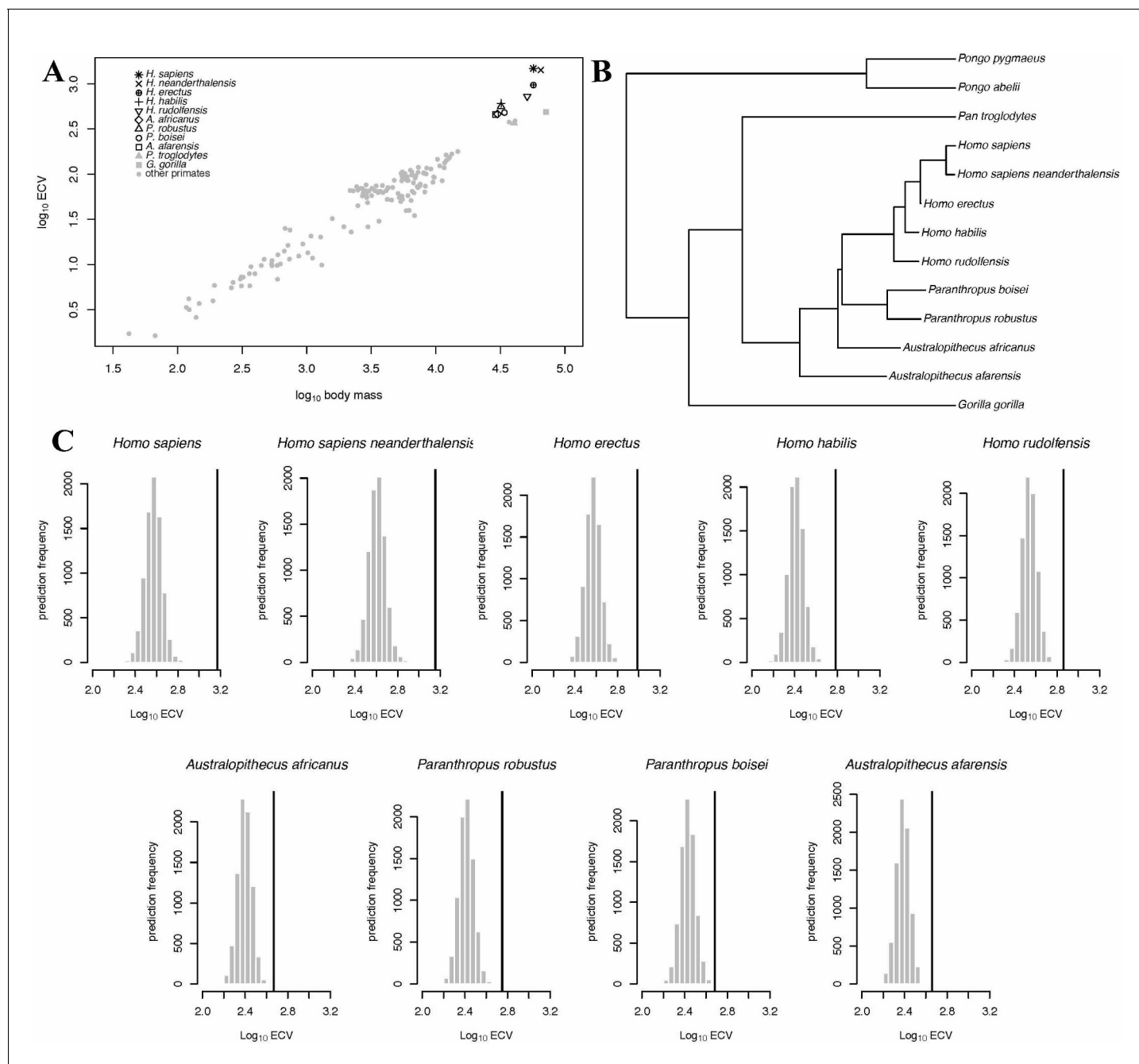
Figure 2—figure supplement 1. BayesModelS predictions of ECV in hominins. Panel (A) shows a scatter plot of primate ECV and body mass data. Panel (B) shows the topology of the great ape portion of the alternate hominin phylogeny used in the BayesModelS analyses of hominin ECV. Panel (C) shows the posterior distributions of predicted ECV values generated by BayesModelS for hominin species with body mass used as the predictor variable. Vertical lines indicated observed values. The observed value for *H. sapiens s* exceeded the mean value predicted by BayesModelS by more than seven standard deviations. All hominin species were strongly supported positive outliers, with >99.9% of predictions falling below the observed values for ECV.

DOI: https://doi.org/10.7554/eLife.41250.009
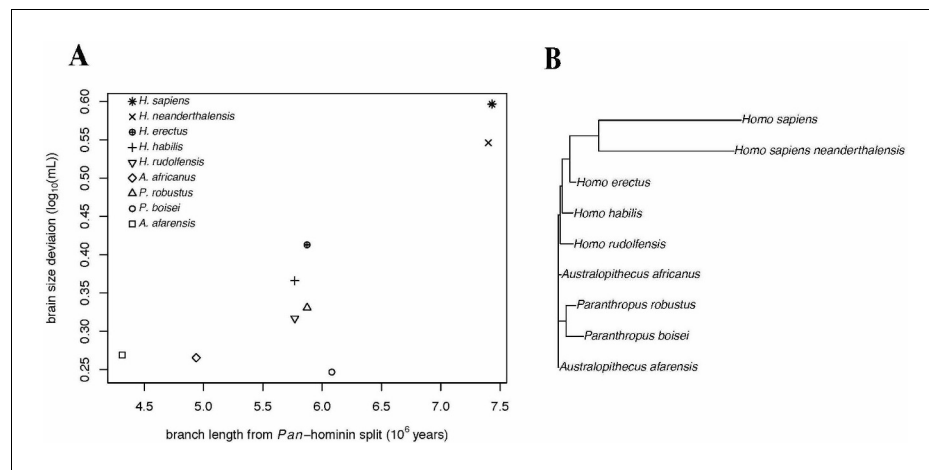
Figure 3. Accelerating Evolution of Brain Size Deviation in Hominins. (**A**) Brain size deviation was calculated as the difference between the mean BayesModelS prediction (made while excluding all hominin data from analysis and using the hominin phylogeny) and the observed value. Phylogenetic distance was measured as time since the shared ancestor of hominins and *Pan* at 7.43 mya. (**B**) Hominin clade in the hominin phylogeny after δ transformation, with δ = 8.36 following the directional acceleration model.
DOI: https://doi.org/10.7554/eLife.41250.013
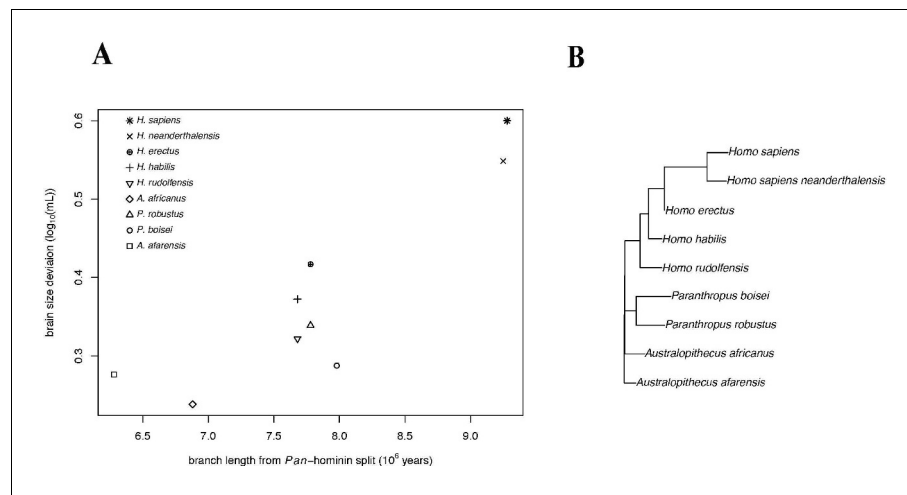
Figure 3—figure supplement 1. Accelerating Evolution of Brain Size Deviation in Hominins (alternate hominin phylogeny). (**A**) Brain size deviation was calculated as the difference between the mean BayesModelS prediction (made while excluding all hominin data from analysis and using the alternate hominin phylogeny) and the observed value. Phylogenetic distance was measured as time since the shared ancestor of hominins and Pan at 9.28 mya. (**B**) Hominin portion of the alternate hominin phylogeny after δ transformation, with δ = 3.745 following the directional acceleration model. Among the PGLS models fit to this data, the directional acceleration model (AICc = −23.88) was favored, as it outperformed the the Brownian (AICc = −15.71), directional (AICc = −22.12), and accelerating (AICc = −22.38) evolution models. This model gave evidence for both evolution towards larger brain volume relative to body mass (slope = 0.06) and for accelerating evolution (δ = 3.745).

DOI: https://doi.org/10.7554/eLife.41250.014
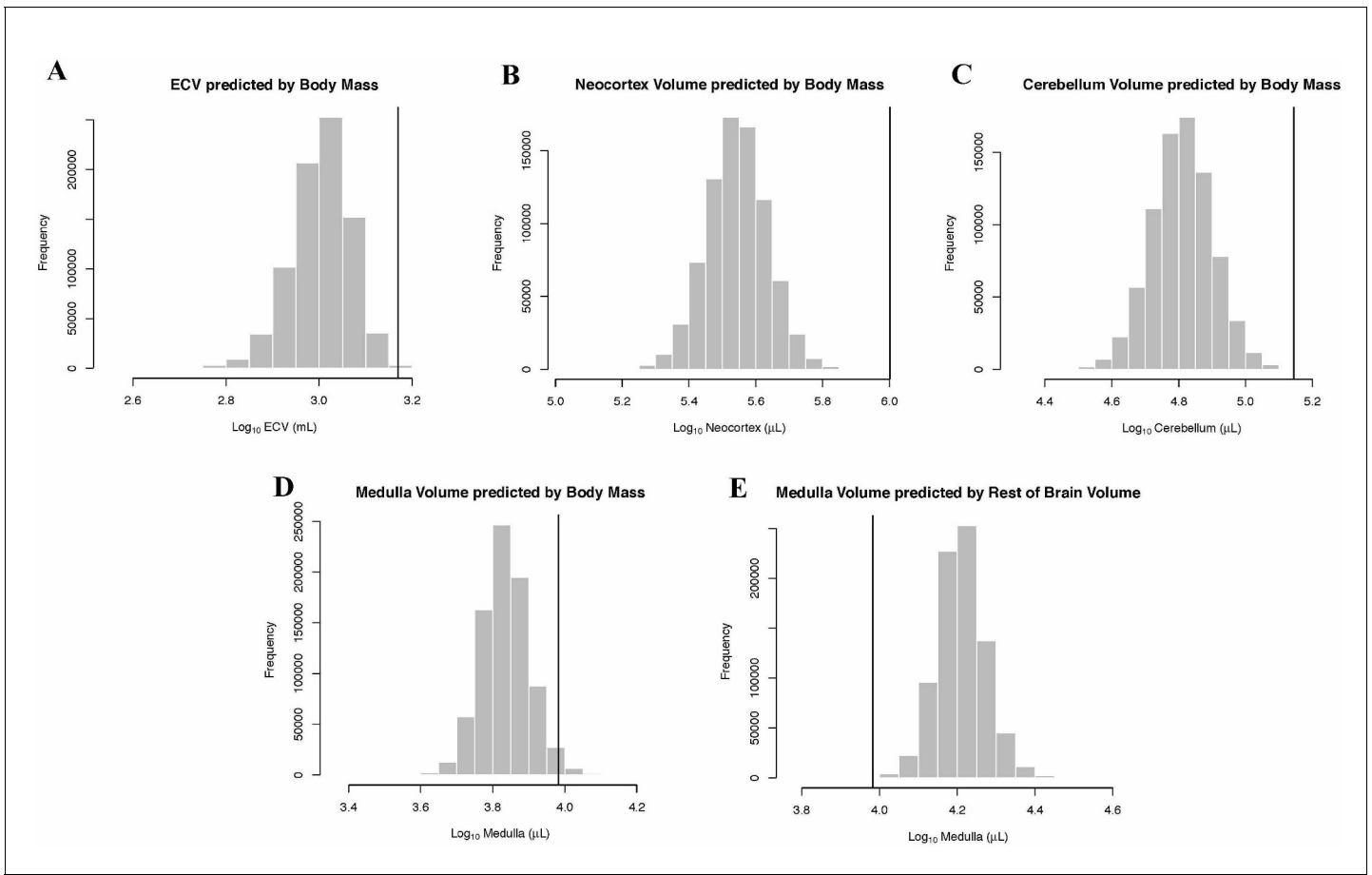
Figure 4. Human Outlier Status for Brain Traits Predicted distributions of trait values generated by BayesModelS are show as histograms. Vertical bars represent the observed values.
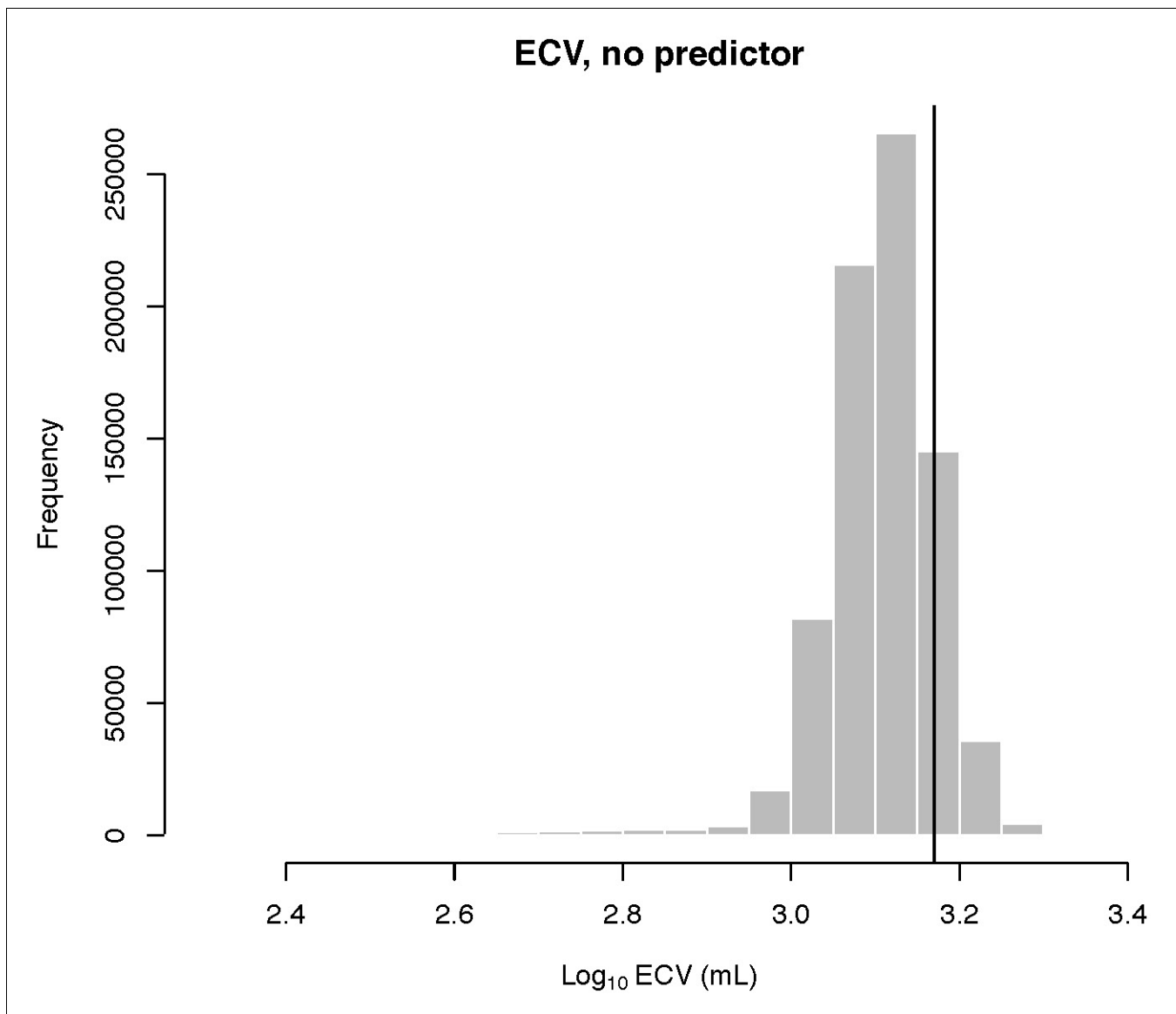
Figure 4—figure supplement 1. Human outlier status for ECV In the BayesModelS analysis of ECV with no predictor variable, humans were not detected as outliers. Results for other species are given in *Source data 1*. Because BayesModelS requires a predictor variable, we assigned each species a random number for the predictor trait. This resulted in the predictor variable not being included in the PGLS model in ~98% of post burn-in MCMC samples. We discarded the remaining samples that included the predictor in the PGLS model before generating predictions.
DOI: https://doi.org/10.7554/eLife.41250.016
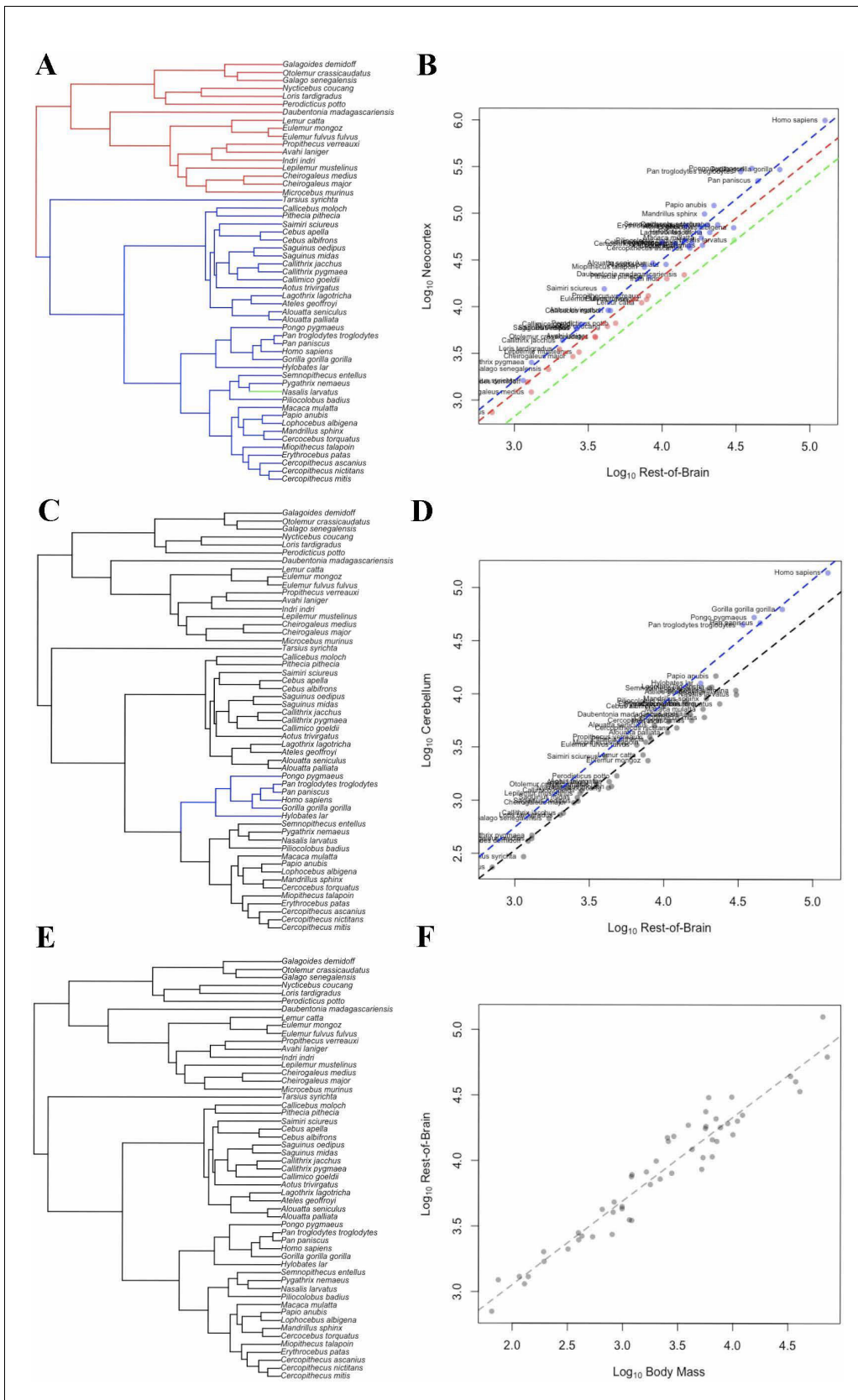
Figure 5. OU Models of Brain Structure Evolution in Primates. (**A and B**) correspond to the OU weighted predictor model of neocortex volume predicted by the rest-of-brain. (**C and D**) correspond to the OU unweighted predictor model of cerebellum volume predicted by the rest-of-brain. (**E**

Figure 5 continued on next page

Figure 5 continued

and **F**) correspond to the OU weighted predictor model of the rest-of-brain volume predicted by body mass. (**A, C**) and (**E**) show the location of selection regimes on the primate phylogeny. (**B, D**) and (**F**) show the optimum regression lines associated with the selection regimes. Points show primate trait and predictor data; colors correspond to the selection regimes. Colors in (**A, C**) and (**E**) match those in (**B, D**) and (**F**).